Available online at www.sciencedirect.com

ScienceDirect

Energy Procedia 38 (2013) 895 – 900

Energy Procedia

SiliconPV: March 25-27, 2013, Hamelin, Germany

Prediction of a double-antireflection coating made solely with SiN_x in a single, directional deposition step

Matthias Winter[a,b]*, Hendrik Holst[a], Pietro P. Altermatt[a]

[a]*Leibniz University Hannover, Institute of Solid-State Physics, Dep. Solar Energy, Appelstr. 2, 30167 Hannover, Germany*
[b]*Institute for Solar Energy Research Hamelin (ISFH), Am Ohrberg 1, 31860 Emmerthal, Germany*

Abstract

Silicon solar cell modules, where the EVA layer is replaced by an air gap, are able to produce the same electric power as standard modules with EVA only if their anti-reflective properties are enhanced. We propose a method to do this by exploiting the fact that, on Si surfaces textured with random pyramids, light incident from near normal angle always hits at least two pyramidal faces before being reflected back toward the sun. If these two faces are covered with an anti-reflective coating (ARC) made of one and the same material but with two different thicknesses, the coating acts as a double ARC. Such a coating can be produced by depositing the SiN_x layer from an oblique angle, optimally from 14.7°. Our detailed raytracing analysis predicts that J_{sc} can then be improved by 0.2 mA/cm^2 for normal incident sunlight and AM1.5g standard illumination, and is improved for all angles within a cone with an apex angle of approximately 64°. Furthermore, the coating can be optimized for modules in vertical mounting, where a J_{sc} gain of 0.1 mA/cm^2 is predicted for an angle of incidence of 40°.

Keywords: ARC ; SiNx ; raytracing ; coating ; air-gap modules

1. Introduction

There have been ongoing efforts to avoid EVA in module fabrication, because EVA contributes to cell efficiency degradation over the long term. Instead of replacing EVA with other materials, a viable option is to replace EVA by an air gap. This creates an additional interface to air at the inner glass surface, which increases reflection, but also improves the transmittance to the solar cell especially in the near ultraviolet. Our raytracing analysis predicts that the loss in short-circuit current density J_{sc} due to the additional glass

* Corresponding author. Tel.: +49-511-762-4850.
E-mail address: winter@solar.uni-hannover.de.

doi:10.1016/j.egypro.2013.07.362

surface and the gain in near ultraviolet light almost cancel out when an anti-reflection coating (ARC) is applied to the inner glass surface. Additionally, the low refractive index of air leaves a wider range of possibilities for improving the ARC properties of the Si cells, while an interface between EVA and silicon has a rather small step in refractive index, making ARCs rather ineffective.

Here, we present a method to reduce the reflectivity at the air/silicon interface for mono-crystalline cells textured with random pyramids without the need of additional manufacturing steps or an additional ARC material. To do this, we exploit the fact that light incident from near normal angle always hits at least two pyramidal faces before being reflected back toward the sun. If these two faces are covered with an ARC made of one and the same material but two different thicknesses, the coating acts as a double ARC.

2. Proposed coating deposition

The proposed type of coating may be achieved by directional deposition of SiN_x from an oblique angle as indicated by θ_D in Fig. 1. This produces, on each pyramid, two faces with a thicker ARC than on the opposite faces. The deposition angle is related to the desired optical thicknesses d_1 and d_2 (measured perpendicularly to the pyramid faces) by

$$\cos\theta_D = \frac{d_1 + d_2}{\sqrt{2(d_1^2 + d_2^2)}}. \quad (1)$$

Here, θ_D is contained in the vertical plane with azimuthal angle $\varphi_D = 0°$, which corresponds to the (010)-plane of the Si lattice. The necessary deposition thickness d_D, i.e. the thickness that would be deposited on a plane target at normal incidence, is calculated by

$$d_D = \sqrt{\frac{3}{2}(d_1^2 + d_2^2)}. \quad (2)$$

Equations (1) and (2) assume a totally directional deposition process without divergence. Depending on the setup, divergence and possibly nondirectional background processes must be taken into account and will lead to different deposition angles.

3. Ray tracing model

For all ray-tracing simulations we assume a mono-crystalline silicon solar cell with a surface textured by random pyramids. The ARC is made of SiN_x with a refractive index of 2.05 (at 633 nm wavelength) as is standard in industry. The rear of the 180 µm thick silicon wafer is fully covered with Al and is assumed to reflect light in a Lambertian manner. We use the AM1.5g spectrum, impinging from an angle of incidence θ as indicated in Fig. 1. Here, we assume a solar cell without any glass cover and compare between the known homogeneous coating and the proposed coating with heterogeneous thickness.

We use the Monte Carlo based ray tracer *Daidalos*, which we recently developed ourselves [1]. We use a simulation domain containing a single pyramid, as has been successfully done for decades. The random pyramid structure is approximated by randomly shifting the light ray horizontally when it hits either a side boundary of the domain or the Al back surface.

While a ray tracer only determines the absorbance spectra $A(\lambda)$, we are interested in the short-circuit current density $J_{sc} = \int_0^\infty A(\lambda)\eta_c(\lambda)\mathrm{d}\lambda$. The collection efficiency $\eta_c(\lambda)$ is obtained from numerical device simulations of a standard industrial cell, using Sentaurus [2]. To increase the accuracy of the simulated J_{sc} the number of rays per wavelength is not only related to the intensity of the AM1.5g spectrum, but is also

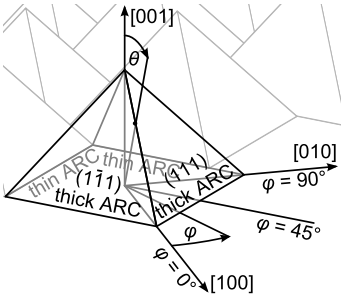

Fig. 1 Crystallographic directions and angle convention used in this paper.

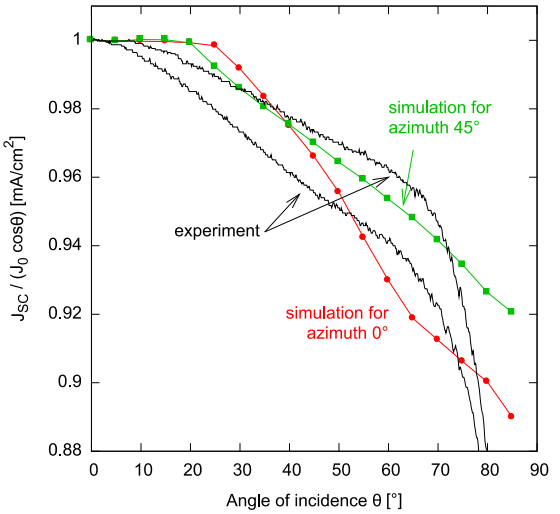

Fig. 2 Simulated J_{sc} (devided by J_{sc} at normal incidence, and by cos θ) in dependence of the incident angle of light θ (symbols) compared to experimental data (lines, from ref. [3]).

multiplied by $\eta_c(\lambda)$. Simulations are performed for wavelengths from 300 through 1200 nm in steps of 10 nm.

4. Angular dependence of J_{sc}

Fig. 2 shows the simulated J_{sc} in dependence of the incident angle θ with two different azimuth angles φ (symbols). Note that the pyramidal structure causes J_{sc} to diverge from the geometric cosine law. Our simulations (symbols) compare reasonably well to measurements (lines) that were performed in Ref. [3] on two cells from two different manufacturers.

The first striking feature of a heterogeneous coating is that the light, hitting first the thick and then the thin coating, or vice versa, suffers different amounts of reflection. Fig. 3 shows such differences for normal incidence light reflected off two adjacent pyramid faces (see inset of Fig. 3). These spectra are not raytraced, but calculated analytically taking only the indicated reflection paths into account. Both paths show two minima in reflectivity, which is the typical behavior of a double ARC. The wavelength interval between both minima is smaller if the thick ARC is hit first than the other way around. This difference arises because the effective thickness varies with the angle of incidence. Combined, both path result in a lower reflectivity in the ultraviolet and infrared which outweighs the increased reflectivity in the visible range. The photon flux is scaled such that for each curve shown the number of incident photon flux amounts to 1000 W/m^2 of the AM1.5g spectrum. The photocurrent is the photon flux multiplied by the elementary charge.

The second striking feature of a heterogeneous coating is that, unlike for homogeneous coatings, $J_{sc}(\theta)$ behaves asymmetrically for positive and negative angle of incidence θ. This is a direct consequence of the asymmetry in the reflection paths. Only for light incident from angles with azimuth $\varphi = \pm 90°$ the ARC behaves symmetrically. The $\varphi = 0°$ direction is the most asymmetrical.

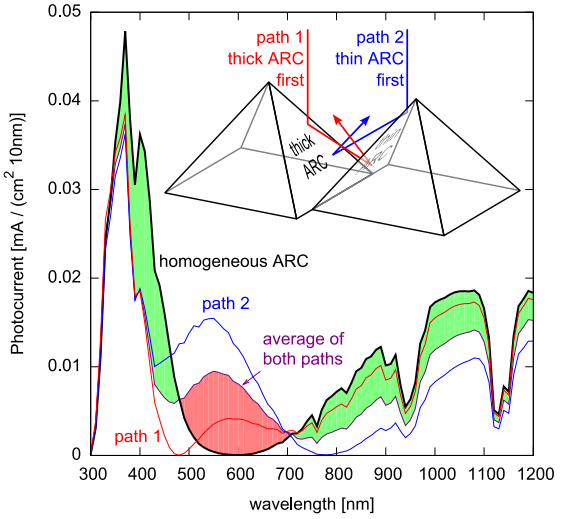

Fig. 3 Calculated spectra reflected off two adjacent pyramid faces. The inset shows the light paths assumed. The initial number of photons is set to be 1000 W/m^2 for each curve. Shaded areas mark the gains and losses compared to a homogeneous ARC (thick line).

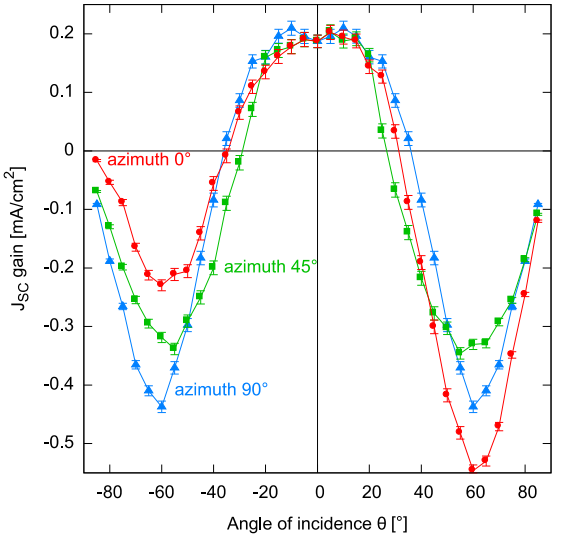

Fig. 4 Simulated J_{sc} in dependence of the incident angle θ, plotted as difference between homogeneous and heterogeneous ARCs. The heterogeneous ARC shown here is optimized for normal incidence.

Table 1 Optimized parameters. The azimuthal deposition angle is always $\varphi_D = 0°$.

ARC	Optical Thickness [nm]		Deposition angle θ_D [°]	Deposition thickness d_D [nm]
	thick areas d_1	thin areas d_2		
Homogeneous	72.7	72.7	0	125.9
Heterogeneous, optimized for normal incidence	99.6	58.2	14.7	141.3
Heterogeneous, optimized for 40° incidence	85.0	55.3	12.0	124.2

5. Improvement in J_{sc}

Our ray-tracing simulations show differences in J_{sc} between a heterogeneous ARC and the standard homogeneous ARC for different angles of incidence which are displayed in Fig 4. For this comparison the thicknesses of the ARCs are chosen to give the highest possible J_{sc} at normal incidence. The optimization can be done by the raytracer, but the accuracy is limited by the statistical error of the Monte Carlo method and the simulation time available. Therefore we use analytical calculations to optimize for normal incidence, which yields accurate results within seconds. For this the probabilities and angles for different reflection paths where taken from Ref. [4]. The result of the optimization is shown in Table 1.

The heterogeneous ARC increases J_{sc} by 0.2 mA/cm^2 at angles close to normal incidence. This is more than a third of what is lost by removal of the EVA from the module and applying an ARC at the inner surface of the glass layer and half of the value which can be reached by a regular double ARC. Since a large part of the improvement arises from the utilization of UV light the improvement which can be reached in EVA encapsulated modules using the proposed method is almost two orders of magnitude less.

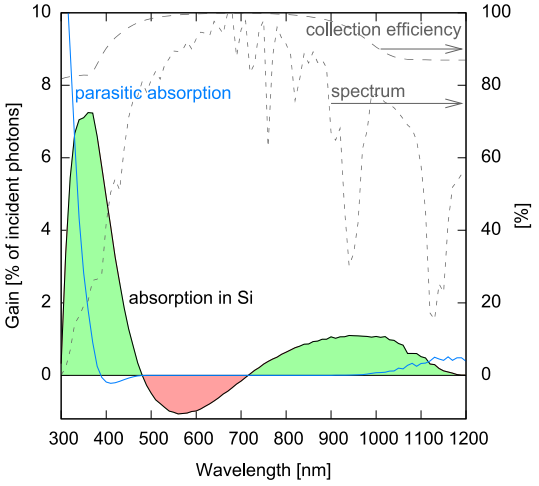

Fig. 5 Simulated difference in absorption between homogeneous and heterogeneous coating in dependence of wavelength. The collection efficiency (dashed line) and the AM1.5g spectrum (dotted line) are drawn to the right axis for reference.

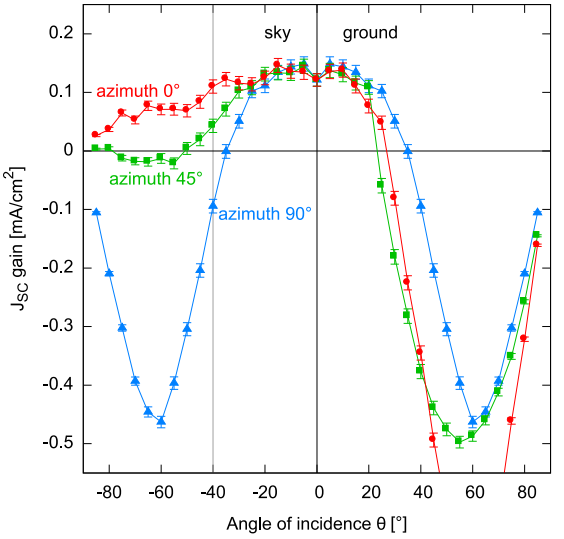

Fig. 6 Angle dependence of the simulated difference in J_{sc} between homogeneous and heterogeneous ARCs. The heterogeneous ARC is optimized for light incident at $\theta = 40°$, suitable in a module mounted vertically, where light impinges always from a negative angle of incidence.

From Fig. 4 it is also apparent that the heterogeneous ARC outperforms the homogeneous ARC in a cone within about $\theta = \pm 32°$ (from $\theta = 27°$ for $\varphi = \pm 45°$ to $\theta = 36°$ for $\varphi = \pm 90°$). Fig. 5 shows the spectral resolution of the gain of the optimized heterogeneous ARC compared to the standard ARC. When compared to the normalized photon flux from the AM1.5g spectrum (dotted line) and the collection efficiency (dashed line), there is a gain in J_{sc} of 0.31 mA/cm^2 in the ultraviolet and infrared, which exceeds the loss of 0.11 mA/cm^2 in the visible light. The difference in reflectivity is just the negative of the difference in absorption reduced by the parasitic absorption. The difference in parasitic absorption contains absorption in the SiN_x of the ARC (short wavelengths) and the Aluminum back surface (long wavelengths). The absorption in the Al is larger for the heterogeneous coating because there is more infrared light entering the cell in the first place. For wavelength below 380 nm there is a strong increase in absorption in the thick part of the heterogeneous coating due to interference effects.

Solar modules which are mounted vertically receiving almost no normal incident light. The asymmetric behavior of the heterogeneous ARC in $\varphi = 0°$ direction can be exploited to optimize the ARC for oblique incidence. Fig. 6 shows the results for a cell optimized for a polar angle of 40°. This optimization was done using the raytracer and the results are included in Table 1. This leads to a gain in J_{sc} for photons coming from most of the sky (negative θ).

6. Summary

The reflectivity at the air/silicon interface of a solar cell textured with pyramids can be enhanced by using a new type of anti-reflection coating (ARC). This coating exploits the fact that light incident from near normal angle always hits at least two pyramidal faces before being reflected back toward the sun. If these two faces are covered with an ARC made of one and the same material but two different thicknesses, the

effect of the coating is similar to a double-ARC. The proposed coating can be achieved by directional deposition from an oblique angle.

This heterogeneous ARC raises the short-circuit current density J_{sc} by 0.2 mA/cm^2 compared to a homogeneous coating for normal incidence under standard conditions. The gain decreases for higher polar angle of incidence. The maximum polar angle for which J_{sc} is increased depends on the azimuth and lies between 27° and 36°. The reflectivity of visible light is increased while the improvement arises from a reduced reflectivity for ultraviolet and infrared light.

The reflectivity differs depending on which ARC thickness is hit first by a ray of light. This leads to an asymmetric behavior of the ARC with respect to the polar angle of incidence. This asymmetry can be utilized to produce an ARC optimized for oblique incidence, e.g. for vertically mounted modules. Optimization for an angle of incidence of 40° results in an improvement of J_{sc} of 0.1 mA/cm^2 for this angle. If such a module is mounted vertically the anti-reflection properties will be improved for light from more than half of the sky.

References

[1] H. Holst, M. Winter, M. R. Vogt, K. Bothe, M. Köntges, R. Brendel and P. P. Altermatt, "Application of a new ray tracing framework to the analysis of extended regions in Si solar cell modules," *Energy Procedia,* vol. 33, 2013.

[2] *Sentaurus Version G-2012.06,* Synopsys Inc., Mountain View, CA.

[3] J. L. Balenzategui and F. Chenlo, "Measurement and analysis of angular response of bare and encapsulated silicon solar cells," *Solar Energy Materials & Solar Cells,* vol. 86, pp. 53-83, 2005.

[4] S. C. Baker-Finch and K. R. McIntosh, "Reflection of normally incident light from silicon solar cells with pyramidal texture," *Prog. Photovolt: Res. Appl.,* vol. 31, 2011.